Available online at www.sciencedirect.com
ScienceDirect
European Journal of Medicinal Chemistry 42 (2007) 334–343
EUROPEAN JOURNAL OF MEDICINAL CHEMISTRY
http://www.elsevier.com/locate/ejmech

Original article

Identification of novel short chain 4-substituted indoles as potent $\alpha_v\beta_3$ antagonist using structure-based drug design

Pierre Raboisson*, Renee L. DesJarlais, Rolanda Reed, Jennifer Lattanze, Margery Chaikin, Carl L. Manthey, Bruce E. Tomczuk, Juan José Marugán

Drug Discovery, Johnson & Johnson Pharmaceutical Research and Development, L.L.C., 665 Stockton Drive, Exton, PA 19341, USA

Received 31 May 2006; received in revised form 16 October 2006; accepted 19 October 2006
Available online 20 December 2006

Abstract

The vitronectin receptor $\alpha_v\beta_3$ has been identified as a promising potential target for the treatment of osteoporosis, diabetic retinopathy and cancer. We have recently reported 5-substituted indoles 3-[5-[2-(5,6,7,8-tetrahydro[1,8]naphthyridin-2-yl)ethoxy]indol-1-yl]-3-(3-pyridyl)propionic acid **3** and 3-[5-[2-(5,6,7,8-tetrahydro[1,8]naphthyridin-2-yl)ethoxy]indol-1-yl]-3-(3,4-methylenedioxyphenyl)propionic acid **4**, as an original series of potent $\alpha_v\beta_3$ antagonists with subnanomolar activity. Ligand–protein docking analyses have been performed to generate binding models of three different chemical classes of known $\alpha_v\beta_3$ antagonists with $\alpha_v\beta_3$. Results of this docking study suggested that indoles bearing the basic tetrahydronaphthyridine group at position 4 can easily adopt the correct binding conformation and should be as potent as our current 5-substituted indole leads **3** and **4**. This hypothesis was nicely demonstrated by the synthesis of a series of 1,4-disubstituted indoles through a tandem of reactions involving: (i) the *N*-alkylation of indoles **15** and **22** with propargyl esters and cesium fluoride, and (ii) a Heck coupling reaction between 4-bromoindole and 7-vinyl-3,4-dihydro-2*H*-[1,8]naphthyridine-1-carboxylic acid *tert*-butyl ester **12**, or (iii) a reductive amination involving the *N*-substituted-4-aminoindole **23** and the BOC-protected tetrahydro[1,8]naphthyridine aldehyde **13**. Among the compounds assayed, 3-(3-pyridyl)-3-[4-[2-(5,6,7,8-tetrahydro[1,8]naphthyridin-2-yl)ethyl]indol-1-yl]propionic acid **21** showed the most promising activity on $\alpha_v\beta_3$ ($IC_{50} = 0.5$ nM), and was found to have the same potency as our current leads **3** and **4**, while maintaining selectivity over $\alpha_{IIb}\beta_{IIIa}$. Moreover, based on the reasonable apparent permeability coefficient in an in vitro CACO-2 cell monolayer assay (P_{app} apical/basolateral $= 2.2 \times 10^{-6}$ cm/s, P_{app} basolateral/apical $= 2.5 \times 10^{-6}$ cm/s), compound **21** is expected to be absorbed through the intestine in human. Thus, 1,4-disubstituted indole **21** represents a new lead for this novel class of conformationally restricted $\alpha_v\beta_3$ antagonists. Additionally, this study validates the pharmacophore model previously postulated and provides an improved basis for further structure-based drug design in the field of $\alpha_v\beta_3$.

Keywords: Integrin; $\alpha_v\beta_3$; $\alpha_v\beta_5$; Indole; Modeling

1. Introduction

The transmembrane vitronectin receptor, $\alpha_v\beta_3$ integrin, is a member of the heterodimeric integrin superfamilly. Since upregulation of the vitronectin receptor, $\alpha_v\beta_3$, has been associated with various pathologies including osteoporosis [1], arthritis [2], and metastatic cancer [3,4], $\alpha_v\beta_3$ antagonist have been recognized as emerging potential therapeutic treatment for various diseases [1,2,4]. Thus, $\alpha_v\beta_3$ integrin antagonists, among them Cilengitide [5,6] and SB273005 [7] (Chart 1) are undergoing clinical evaluation as cancer and osteoporosis treatment. We have recently described the identification of the 3-[5-[2-[6-(methylamino)-2-pyridyl]ethoxy]indol-1-yl)-propanoic acid **1** (Chart 1), an orally active $\alpha_v\beta_3$ receptor antagonists incorporating the indole bicycle as the central template [8]. In subsequent work, it was advantageously found that the use of the guanidinomimetic tetrahydronaphthyridine (THN) surrogate as the basic ending together with the substitution of the β-position with an aromatic group (e.g. phenyl,

* Corresponding author. Present address: Department of Medicinal Chemistry, Tibotec BVBA (Division of JNJ), Gen. De Wittelaan L 11B 3, 2800 Mechelen, Belgium. Tel.: +32 1544 4262; fax: +32 1540 1257.
E-mail address: pierreraboisson@aol.com (P. Raboisson).

0223-5234/$ - see front matter © 2006 Elsevier Masson SAS. All rights reserved.
doi:10.1016/j.ejmech.2006.10.015

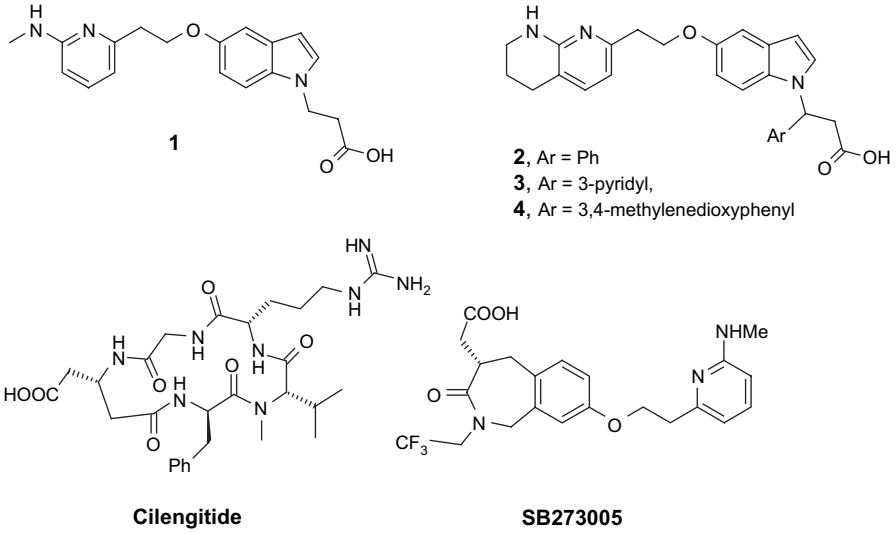

Chart 1. Reference $\alpha_v\beta_3$ antagonists: Cilengitide, SB273005 and in-house lead compounds (**1**–**4**).

3-pyridyl, and methylenedioxyphenyl) of the propionic acid of compound **1** dramatically improved the potency of the resulting compounds [8,9]. This finding led to the identification of lead compounds **2**–**4** [9] as potent $\alpha_v\beta_3$ antagonists mimicking the RGD triad [10] of the natural ligand vitronectin.

In order to better understand the structure–activity relationship studies around this series of compounds, we decided to explore the binding mode of these zwitterionic structures through a docking model using the recently reported X-ray structure of $\alpha_v\beta_3$ integrin [11,12]. Herein, we report the results of the study developed with detailed structural information on the interaction between $\alpha_v\beta_3$ integrin receptor and its ligands together with our in-house pharmacophore hypotheses, which has successfully led to the development of novel potent $\alpha_v\beta_3$ antagonists.

2. Methodology

Compounds **2**, **5**–**9** (Chart 2) were built in MacroModel 7.0 [13] and minimized with the MMFFs force field [14–20]. For compounds **2**, **7** and **8**, the stereochemistry of the active isomer is not known. For the modeling studies, it is assumed to be the same as for compound **5**, as this ultimately provides the best fit to the $\alpha_v\beta_3$ RGD binding site. These structures were then read

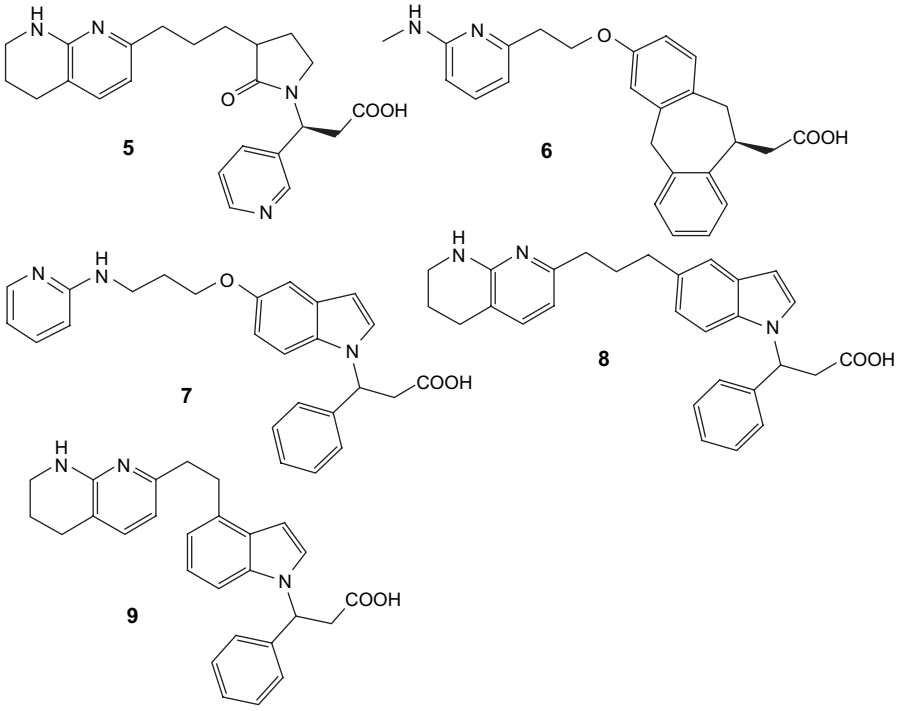

Chart 2.

into InsightII [21] along with the $\alpha_v\beta_3$/cyclic RGD-containing peptide crystal structure, PDB ID 1L5G [11], which was obtained from the Protein Data Bank [12]. For each molecule, the carboxyl group was overlaid on the carboxyl of the aspartate in the cyclic peptide. Torsion angles of each molecule were adjusted to provide hydrogen bonds similar to those made by the guanidine group in the cyclic peptide and avoid contact with the $\alpha_v\beta_3$ protein. The torsional preferences of the O-linked compound **2** and the C-linked compound **8** were estimated using semi-empirical quantum mechanics on the model systems methoxybenzene and ethylbenzene. The torsion angle was sampled every 30 degrees between 0 and 180 with geometry optimization at each angle using the AM1 parameterization [22] in PC Spartan [23].

3. Results

Based on the crystal structure of $\alpha_v\beta_3$ and an RGD peptide [11], important interaction sites for the RGD can be identified. The aspartate carboxyl group makes hydrogen bonds to the backbone NH of N215 on β_3 and serves as a ligand for a protein-bound metal, manganese in the crystal and magnesium in vivo. The guanidine of the arginine makes two hydrogen bonds to D218 and a third to D150, both on α_v. The glycine and the backbone do not make any additional interactions with the protein. The phenylalanine, following the aspartate in the cyclic peptide, is near Y122 of the β_3 protein. Although this does not appear to be a well-defined pocket, antagonists gain potency by providing an aromatic or hydrophobic group to mimic the phenylalanine side chain.

Fig. 1a illustrates the interactions between the peptide and $\alpha_v\beta_3$ using the available crystal structure, 1L5G [11]. The non-peptidic $\alpha_v\beta_3$ ligands employed in the present study (compounds **2**, **5**–**9**) are depicted in Chart 2. A schematic representation of the proposed binding mode of the lead compound **9** is depicted in Fig. 1b. As shown in Fig. 1b and 1c, all the new compounds **2**, **5**–**9** mimic the interactions of the aspartate, phenylalanine, and partially the guanidine. The fact that many scaffolds can be used to present these interacting groups goes along with the observation in the crystal structure that the glycine and peptide backbone do not make interaction with $\alpha_v\beta_3$. The importance of the scaffold appears to be the ability to present the aspartate and guanidine mimetics in the correct orientation for recognition by $\alpha_v\beta_3$. This observation dates to early NMR studies of cyclic peptides [24,25] and has been consistently reinforced by the SAR in a wide variety of $\alpha_v\beta_3$ antagonists [26–28].

In our own series, the difference in activity between compounds **2** (IC_{50} ($\alpha_v\beta_3$) = 1.0 nM) and **8** (IC_{50} = 14 nM) can be explained using this docking model. The energies of model compounds obtained from the quantum mechanics calculations were plotted versus the torsion angle in the final geometry optimized structure (Fig. 2). This analysis shows that methoxy and ethylbenzene have opposite energy preferences. The methoxy prefers to be in the plane while the ethyl prefers to be out of the plane. The predicted bound conformations of the compounds **2** and **8** show that the linker needs to be close

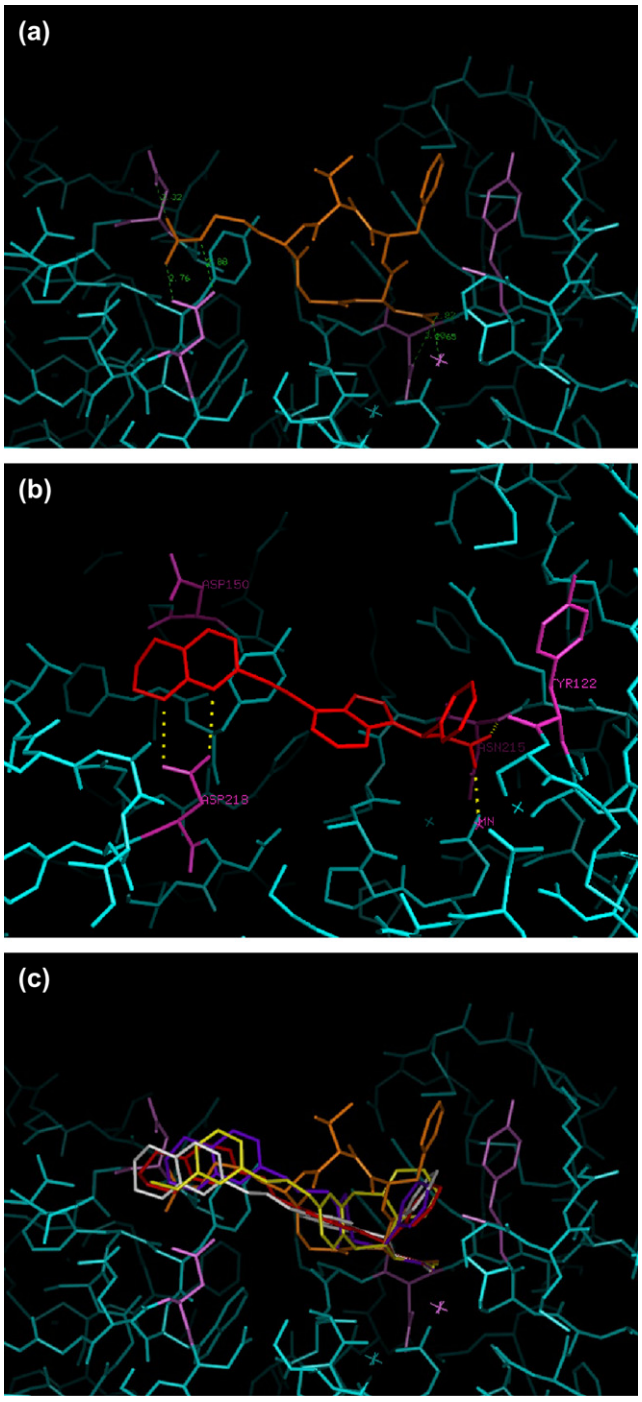

Fig. 1. (a) Crystal structure of $\alpha_v\beta_3$ and VRGDdF cyclic peptide [22]. The crystal structure of $\alpha_v\beta_3$ in cyan with residues providing important interactions in magenta and VRGDdF cyclic peptide in orange [11] is shown with important interactions highlighted with dotted lines. (b) Schematic representation of compound **9** bound to the binding site of $\alpha_v\beta_3$. (c) Superimposition of $\alpha_v\beta_3$ antagonists **2**, **5**–**9** in the ligand-binding site of $\alpha_v\beta_3$. Models of compounds **5** in purple, **6** in yellow, **9** in red and **2** in white are shown with the crystal structure of $\alpha_v\beta_3$ in cyan with residues providing important interactions in magenta and VRGDdF cyclic peptide in orange [11]. Models for compounds **8** and **7** are nearly identical to the model for compound **2**. (For interpretation of the references to colours in figure legends, the reader is referred to the web version of this article.)

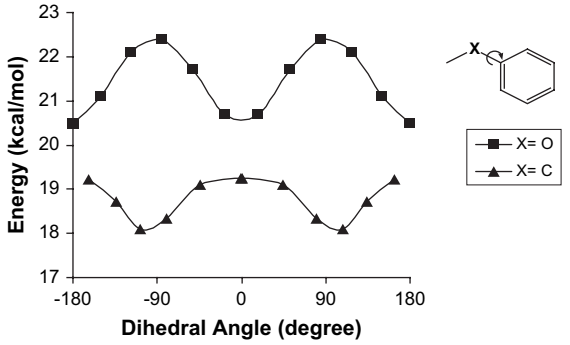

Fig. 2. Graph of energy versus the indicated dihedral angle for methoxybenzene (X = O) and ethylbenzene (X = C).

to the plane. Since the energy difference between 0 and 90 degrees is about 1 kcal/mol, the carbon linked analog would be expected to be less active by this amount. Thus, most of the difference in activity between compounds **2** and **8** (approximately 14-fold) can be accounted for 1 kcal/mol increase in conformational energy for the methylene linker of compound **8** on binding to $\alpha_v\beta_3$. Compound **2** binds very close to its minimum energy with respect to the oxygen linker conformation.

Interestingly, the overlay of compound **2** with the cyclic peptide led to the hypothesis that a compound that was substituted at the 4-position of the indole ring which uses a shorter linker (e.g. compound **9**) could achieve the same interaction and potentially provide a novel series of potent $\alpha_v\beta_3$ antagonists. As seen in Fig. 3, modeling of the proposed compound **9** supported this assumption. With the aim of verifying this hypothesis, we synthesized and biologically evaluated indoles **9**, **21** and **26** for their potency and selectivity profile toward $\alpha_v\beta_3$.

4. Chemical synthesis

The two tetrahydronaphthyridine intermediates **12** and **13** were synthesized according to the procedure outlined in Scheme 1. The alcohol **10** [9] was converted to the corresponding iodo derivative **11** with iodine, imidazole and triphenylphosphine in 89% yield. Treatment of **11** with potassium *tert*-butoxide afforded the olefin **12**, which was cleaved by ozonolysis to give the aldehyde **13** in 57% yield.

The key intermediate **15** in the synthesis of 1,4-disubstituted indoles **9** and **21** was obtained by a Heck coupling reaction between the commercially available 4-bromoindole **14** and BOC-protected 7-vinyl-1,2,3,4-tetrahydronaphthyridine olefin **12** as shown in Scheme 2. The resulting alkene **15** was then alkylated through a Michael addition using phenylpropargylate ethyl ester and cesium fluoride to afford the 1-substituted indole

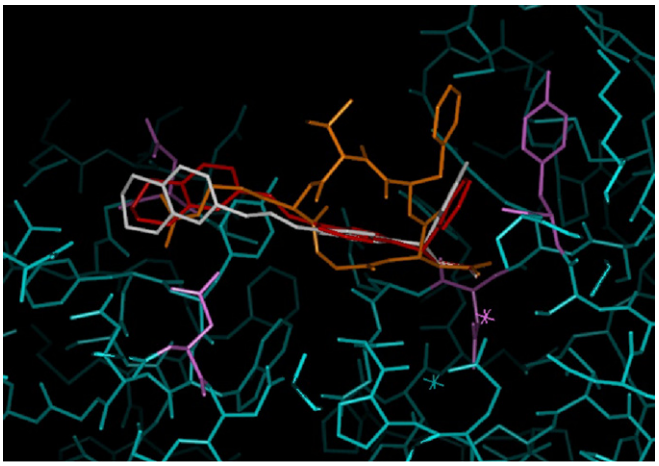

Fig. 3. Models of compounds **2** in white and **9** in red are shown with the crystal structure of $\alpha_v\beta_3$ in cyan with residues providing important interactions in magenta and VRGDdF cyclic peptide in orange [11].

16. Hydrogenation under palladium catalysis of **16** followed by the deprotection of the BOC group using copper(I) triflate and subsequent saponification of the ester **18** yielded target final product **9** in 73% yield. In a similar manner, intermediate **15** was first alkylated with 3-pyridylpropargylate methyl ester, using the standard cesium fluoride procedure, leading to **19** (84% yield). The ester **19** was simultaneously saponified with lithium hydroxide and reduced to the target indole **20**, which was subsequently BOC-deprotected with copper(I) triflate to afford the desired final product **21** in 48% yield.

The 4-aminoindole **26** was synthesized through a tandem of reactions involving a Michael addition and a subsequent reductive amination as depicted in Scheme 3. Reaction of commercially available 4-aminoindole **22** with 3-pyridylpropargylate methyl ester and cesium fluoride gave 1-substituted indole derivative **23** in 85% yield. Treatment of **23** with 8-(*t*-BOC)-5,6,7,8-tetrahydronaphthyridine-2-carboxaldehyde and sodium triacetoxyborohydride generated the 4-aminoindole **24** (72% yield). Subsequent saponification and catalytic hydrogenation of ester **24** afforded the acid **25**, which was ultimately BOC-deprotected using the standard copper triflate procedure to afford the final product **26**.

5. Biological activity

Final compounds were evaluated for their binding affinity for $\alpha_v\beta_3$ and $\alpha_v\beta_5$ integrin receptors (ELISA binding assay) and for their selectivity profile toward $\alpha_5\beta_1$ and $\alpha_{IIb}\beta_{IIIa}$ integrins [29–31]. Structure, binding data and comparison to the clinical candidate Cilengitide [5] are recorded in Table 1. In agreement

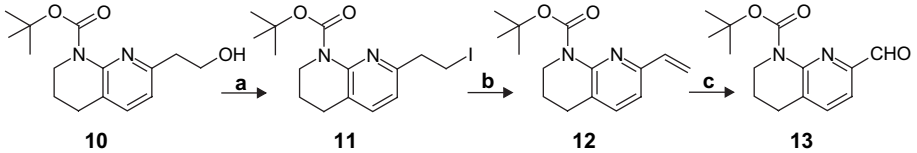

Scheme 1. Synthesis of tetrahydronaphthyridine starting materials **12** and **13**: (a) imidazole, triphenylphosphine, TEA, I_2, CH_2Cl_2, 0 °C–25 °C; (b) *t*-BuOK, THF, −78 °C to r.t.; (c) $NaIO_4$, 4-methylmorpholine-*N*-oxide, OsO_4, CH_3CN, H_2O, r.t.

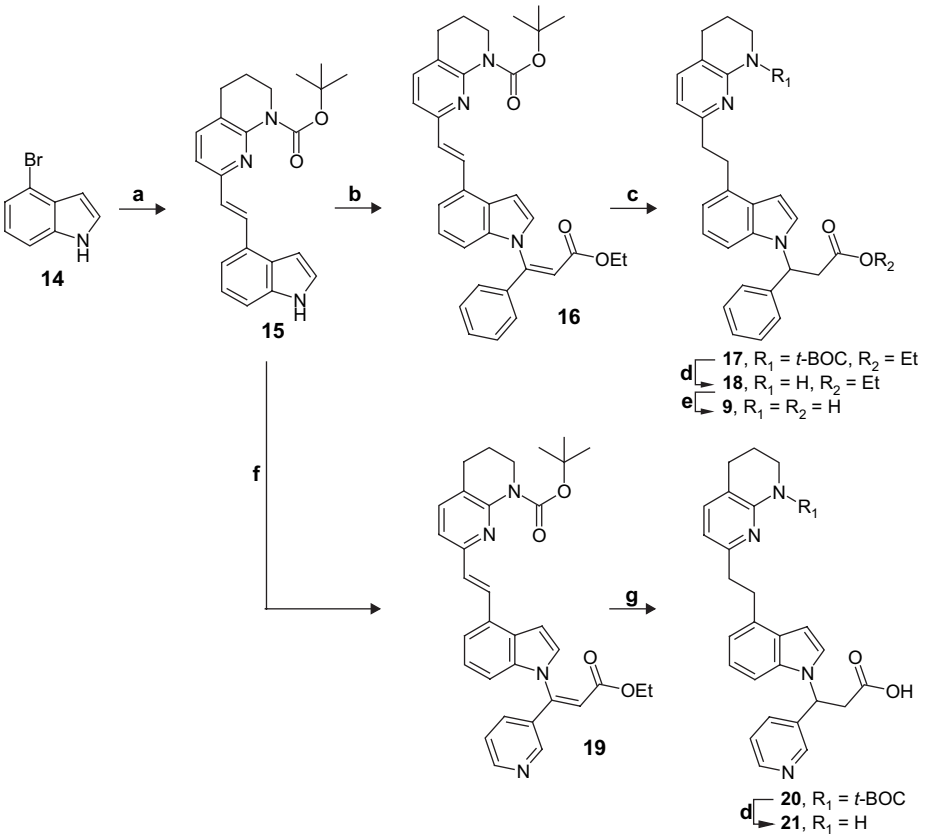

Scheme 2. Synthesis of indoles **9** and **21**: (a) **12**, $Pd(OAc)_2$, tri-*o*-tolylphosphine, TEA, DMF, 110 °C, microwave oven; (b) PhC≡CCOOEt, CsF, DMF, 75 °C; (c) H_2, Pd/C, MeOH; (d) CuTf, toluene, 130 °C, microwave oven; (e) $LiOH \cdot H_2O$, MeOH/THF/H_2O, r.t.; (f) 3-pyridylC≡CCOOEt, CsF, DMF, 75 °C; (g) $LiOH \cdot H_2O$, H_2, Pd/C, MeOH/THF/H_2O, r.t.

with our docking study, compound **9** was found to be equally active as the parent compound **2** (IC_{50} ($\alpha_v\beta_3$) = 0.96 and 1.0 nM, respectively). Moreover, as previously reported [9], the replacement of the phenyl ring of **9** (IC_{50} ($\alpha_v\beta_3$) = 0.96 nM) with a 2-pyridyl (**21**, IC_{50} ($\alpha_v\beta_3$) = 0.50 nM) at the β-position of the propionic acid chain improved by 2-fold the affinity of the resulting compounds for $\alpha_v\beta_3$ integrin. Interestingly, the replacement of the ethylene link between the indole and the THN basic ending of compound **21** with an aminomethyl moiety entailed a loss of affinity on α_v integrins (compare **21**–**26**). This could be explained by the fact that in the binding model of **26** with $\alpha_v\beta_3$, the 4-NH group is approximately at 3.5 Å from the phenyl ring of Y128 on α_v. Thus, the NH would need to be partially desolvated without having a hydrogen bond to the protein, generating the observed loss of activity. Interestingly, the new $\alpha_v\beta_3$ antagonists **9**, **21** and **26** appeared to be equally potent on $\alpha_v\beta_5$, another integrin targeted for the treatment of cancer and osteoporosis [4]. Having demonstrated the validity of

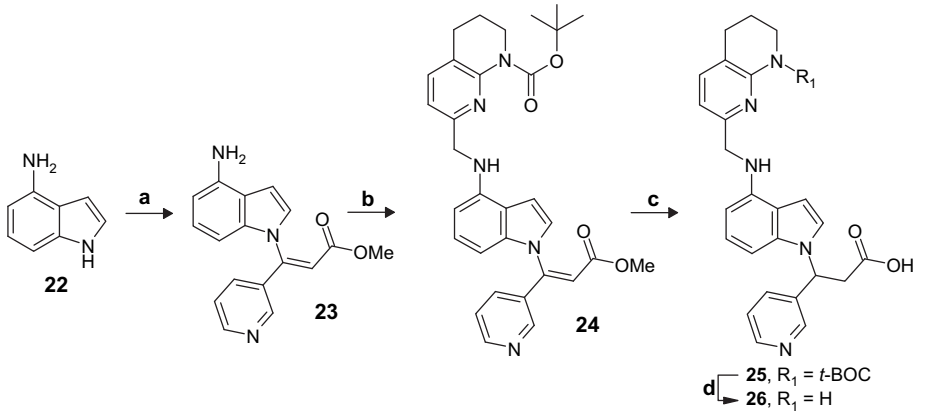

Scheme 3. Synthesis of indole **26**: (a) 3-pyridylC≡CCOOEt, CsF, DMF, 75 °C; (b) **13**, $NaBH(OAc)_3$, AcOH, $C_2H_4Cl_2$, r.t.; (c) $LiOH \cdot H_2O$, H_2, Pd/C, MeOH/THF/H_2O, r.t.; (d) CuTf, toluene, 130 °C, microwave oven.

Table 1

Compound	Integrin IC_{50} (nM)[a]			
	$\alpha_v\beta_3$	$\alpha_v\beta_5$	$\alpha_5\beta_1$	$\alpha_{IIb}\beta_{IIIa}$
Cilengitide [5]	0.86	2.1	14	>1000
2 [9]	1.0	0.68	41	>1000
3 [9]	0.25	0.21	15	>1000
4 [9]	0.38	0.50	24	>1000
8 [9]	14	15	1100	>1000
9	0.96	1.1	107	>1000
21	0.5	0.96	250	>1000
26	4.4	11	9400	>1000

[a] The binding IC_{50} on $\alpha_v\beta_3$ was determined by an ELISA assay as previously reported [30,31].

exchanging the 1,5-disubstituted indole scaffold for the 1,4-disubstituted indole bicycle, while maintaining the potency toward $\alpha_v\beta_3$ and $\alpha_v\beta_5$ integrins, we evaluated this novel series of 4-substituted indole derivatives for their selectivity against other integrins. Because other integrins like the fibrinogen receptor IIbIIIa are implicated in essential phenomena such as blood coagulation [30,31], selectivity of α_v antagonists is essential for their development as drugs. As seen in Table 1, the selectivity of the 4-substituted indole antagonists toward $\alpha_v\beta_3$ and $\alpha_v\beta_5$ versus IIbIIIa was perfectly maintained when compared to the parent compounds **2**–**4**, while the selectivity toward $\alpha_5\beta_1$ was improved. In these assays, **21** was found to be, respectively, 260-fold and 500-fold less active for IIbIIIa and $\alpha_5\beta_1$ than for $\alpha_v\beta_3$. Furthermore, compound **21** was assayed in a CACO-2 cell monolayers assay [32], a potent and widely accepted in vitro model to predict intestinal drug permeability in humans [33]. The apparent permeability coefficient (P_{app}) from the apical to basolateral side was determined to be 2.2×10^{-6} cm/s, while the P_{app} from the basolateral to apical side was found to be 2.5×10^{-6} cm/s. Based on these results, which are in the medium range from our laboratory, compound **21** is expected to have a reasonable gastrointestinal permeability.

6. Conclusion

As a part of our ongoing efforts to optimize our indole-based non-peptide $\alpha_v\beta_3$ integrin antagonists and in order to rationalized our in-house pharmacophore model, computational docking studies using the X-ray structure of the vitronectin receptor bound to the ligand PDB ID 1L5G [11], have been performed. This study led to the identification of a novel class of less flexible 1,4-disubstituted indoles with single digit nanomolar binding affinity for $\alpha_v\beta_3$ and $\alpha_v\beta_5$ receptors. The preferred compound, namely 3-(3-pyridyl)-3-[4-[2-(5,6,7,8-tetrahydro[1,8]naphthyridin-2-yl)ethyl]indol-1-yl]propionic acid **21** showed an IC_{50} values of 0.50 nM for the $\alpha_v\beta_3$ integrin with an improved selectivity over IIbIIIa-fibrinogen receptor ($IC_{50} > 1000$ nM) when compared to the parent leads **2**–**4**, which associated with the favorable cell permeability of **21** justifies further pharmacological studies. Additionally, we demonstrated the usefulness of docking simulations to the vitronectin receptor in suggesting novel analogs and rationalizing SAR trends.

7. Experimental section

7.1. Chemical synthesis

7.1.1. General

Reagents used for the synthesis were purchased from Sigma–Aldrich (Milwaukee-WI, USA) and Lancaster (Windham-NH, USA). All solvents were obtained from commercial suppliers and used without further purification. Flash chromatography was performed on Geduran® Silica gel Si 60 (40–63 μm, Merck). Thin-layer chromatography was carried out using plates Silica gel 60 F_{254} (Merck). The spots were visualized either under UV light ($\lambda = 254$ nm) or by spraying with molybdate reagent (H_2O/concentrated H_2SO_4/$(NH_4)_6Mo_7O_{24}\cdot 4H_2O$/$(NH_4)_2$/$Ce(SO_4)_4\cdot 2H_2O$, 90/10/25/1, v/v/w/w) and charring at 140 °C for a few minutes. All chemical yields are unoptimized and generally represent the result of a single experiment.

^{1}H NMR were recorded on a Bruker B-ACS-120 (400 MHz) spectrophotometer at room temperature. Chemical shifts are given in ppm (δ), coupling constants (J) are in Hertz (Hz) and signals are designated as follows: s, singlet; d, doublet; t, triplet; q, quadruplet; quint., quintuplet; m, multiplet; br s, broad singlet. The LC-MS/MS were determined using an API-2000 triple quadrapole mass spectrometer using the TurboIonspray source, a Shimadzu LC-10ADvp pumping system, a CTC/Leap HTS PAL autosampler, and a C8 LC column (Princeton Chromatography, 5u, 50 × 3.0 mm). The LC-MS data were recorded on a Waters ZQ electrospray mass spectrometer equipped with 4-channel MUX capabilities (Milford, MA) with ELS detection using a Princeton SPHER HTS 60 Å, 5 μm column (3 mm × 50 mm) Princeton Chromatography (Cranbury, NJ). Two mobile phases (A: 99.85% water, 0.1% formic acid, 0.05% TFA; B: 99.9% acetonitrile, 0.1% formic acid, 0.05% TFA) were employed as a gradient from 10% B to 100% B in 4 min with a flow rate of 1.2 mL/min. Accurate mass determination was performed on an Autospec E high-resolution magnetic sector mass spectrometer tuned to a resolution of 6K; the ions were produced in a fast atom bombardment source at 8 kV. Linear voltage scans were collected to include the sample ion and two poly(ethylene glycol) ions, which were used as internal reference standards.

7.1.2. 7-(2-Iodoethyl)-3,4-dihydro-2H-[1,8]naphthyridine-1-carboxylic acid tert-butyl ester (*11*)

To a stirred solution of **10** [9] (25 g, 90 mmol), imidazole (6.9 g, 100 mmol), triphenylphosphine (26.2 g, 100 mmol), and triethylamine (20 mL) in dichloromethane (200 mL) at 0 °C was added iodine (25.3 g, 100 mmol). After 20 min of stirring at 0 °C, the reaction mixture was allowed warm up to 25 °C, then diluted with ethyl acetate, washed with water and diluted $NaHSO_3$, dried (Na_2SO_4), and concentrated to dryness under reduced pressure. Chromatography on silica (AcOEt/hexane, 1:3) afforded **11** (31.0 g, 89%) as a slightly yellow solid. ^{1}H NMR (400 MHz, $CDCl_3$) δ 1.52 (s, 9H, $(CH_3)_3$), 1.91 (quint., $J = 6.4$, 2H, CH_2), 2.73 (t, $J = 6.6$, 2H, CH_2), 3.27 (t, $J = 7.4$, 2H, CH_2), 3.52 (t, $J = 7.4$, 2H, CH_2),

3.76 (t, $J = 6.0$, 2H, CH_2), 6.82 (d, $J = 7.6$, 1H, ArH), 7.33 (d, $J = 7.6$, 1H, ArH); *m/z* 389 $(M + H)^+$.

*7.1.3. 7-Vinyl-3,4-dihydro-2H-[1,8]naphthyridine-1-carboxylic acid tert-butyl ester (**12**)*

Potassium *tert*-butoxide (1.0 M in THF, 80 mL) was slowly added under argon, at −78 °C, to a stirred solution of **11** (31.0 g, 80 mmol) in anhydrous THF (150 mL). After 5 min, the reaction mixture was allowed to warm up to 0 °C, then quenched with silica gel (50 g). Chromatography on silica (EtOAc/hexane, 1:2) yielded **12** (11.0 g, 53%) as white powder. ^{1}H NMR (400 MHz, $CDCl_3$) δ 1.52 (s, 9H, $(CH_3)_3$), 1.92 (quint., $J = 6.4$, 2H, CH_2), 2.74 (t, $J = 6.6$, 2H, CH_2), 3.76 (t, $J = 6.0$, 2H, CH_2), 5.39 (dd, $J = 10.8$, $J = 1.6$, 1H, CH), 6.21 (dd, $J = 17.2$, $J = 1.6$, 1H, CH), 6.72 (dd, $J = 17.2$, $J = 6.8$, 1H, CH), 6.95 (d, $J = 7.6$, 1H, ArH), 7.33 (d, $J = 7.6$, 1H, ArH); *m/z* 261 $(M + H)^+$.

*7.1.4. 7-Formyl-3,4-dihydro-2H-[1,8]naphthyridine-1-carboxylic acid tert-butyl ester (**13**)*

To a solution of **12** (10.4 g, 40 mmol), sodium periodate (34.2 g, 160 mmol), 4-methylmopholine-*N*-oxide (5.2 g, 44 mmol) in acetonitrile (300 mL) and water (150 mL) was added osmium tetroxide (100 mg, 0.40 mmol), and the mixture was stirred at room temperature overnight. Then, solvents were evaporated in vacuo and the residue was partitioned between ethyl acetate (200 mL) and water (150 mL). The aqueous layer was extracted twice with additional ethyl acetate (2 × 50 mL). The combined organic phases were washed with water (70 mL), dried (Na_2SO_4) and concentrated under reduced pressure. The crude material was purified by column chromatography on silica (EtOAc/hexane, 1:2) to give **13** (6.0 g, 57%) as white powder. ^{1}H NMR (400 MHz, $CDCl_3$) δ 1.55 (s, 9H, $(CH_3)_3$), 1.98 (quint., $J = 6.4$, 2H, CH_2), 2.87 (t, $J = 6.6$, 2H, CH_2), 3.82 (t, $J = 6.0$, 2H, CH_2), 7.57–7.63 (m, 2H, ArH), 9.96 (s, 1H, CHO); *m/z* 263 $(M + H)^+$.

*7.1.5. 7-[2-(1H-Indol-4-yl)vinyl]-3,4-dihydro-2H-[1,8]naphthyridine-1-carboxylic acid tert-butyl ester (**15**)*

A solution of 4-bromoindole (467 mg, 2.38 mmol), **12** (620 mg, 2.38 mmol), $Pd(OAc)_2$ (43 mg, 0.192 mmol), tri-*o*-tolylphosphine (172 mg, 5.65 mmol), and triethylamine (1.3 mL, 9.33 mmol), in dimethylformamide (6 mL) was stirred at 110 °C for 18 min in a multimods Smith synthesizer® microwave oven equipped with a probe that regulate the temperature in the reaction medium along with a built-in magnetic stirrer. After the mixture was cooled at room temperature, the solvent was evaporated in vacuo. Then, the residue was partitioned between AcOEt and water. The organic layer was dried (Na_2SO_4) and concentrated under reduced pressure. The crude material was purified by column chromatography on silica (EtOAc/CH_2Cl_2, 1:1) yielded **15** (560 mg, 63%). ^{1}H NMR (400 MHz, DMSO-d_6) δ 1.50 (s, 9H, $(CH_3)_3$), 1.86 (quint., $J = 6.3$, 2H, CH_2), 2.74 (t, $J = 6.4$, 2H, CH_2), 3.69 (t, $J = 6.0$, 2H, CH_2), 6.78 (br s, 1H, NH), 7.14 (t, $J = 7.8$, 1H, ArH), 7.22 (d, $J = 8.0$, 1H, ArH), 7.32 (d, $J = 15.6$, 1H, CH), 7.33 (d, $J = 7.6$, 1H, ArH), 7.38 (d, $J = 8.0$, 1H, ArH), 7.47 (t, $J = 2.8$, 1H, ArH), 7.51 (d, $J = 8.0$, 1H, ArH), 8.00 (d, $J = 15.6$, 1H, CH), 11.3 (s, 1H, ArH); *m/z* 276 $(M - (t\text{-BOC}) + H)^+$.

*7.1.6. 7-[2-[1-(2-Ethoxycarbonyl-1-phenylvinyl)-1H-indol-4-yl]vinyl]-3,4-dihydro-2H-[1,8]naphthyridine-1-carboxylic acid tert-butyl ester (**16**)*

To a solution of **15** (560 mg, 1.49 mmol) and ethylphenylpropiolate (369 μL, 2.24 mmol) in dry DMF (3.5 mL) was added cesium carbonate (300 g, 1.98 mmol), and the mixture was heated at 75 °C for 1.5 h. After the mixture was cooled at room temperature, the solvent was evaporated in vacuo. Then, the residue was partitioned between ice-cold water (50 mL) and ether (70 mL). The aqueous layer was extracted twice with additional ether (2 × 50 mL) and dried (Na_2SO_4). After evaporation of the solvent, the residue was chromatographed on silica (EtOAc/hexanes, 1:3–1:1) to give **16** (475 mg, 58%). ^{1}H NMR (400 MHz, $CDCl_3$) δ 0.91–0.93 (m, 1.5H, ½CH_3), 1.38–1.42 (m, 1.5H, ½CH_3), 1.60 (s, 9H, $(CH_3)_3$), 1.96–2.00 (m, 2H, CH_2), 2.78–2.82 (m, 2H, CH_2), 3.82–3.85 (m, 2H, CH_2), 3.97–4.02 (m, 1H, ½CH_2), 4.11–4.16 (m, 1H, ½CH_2), 6.23 (s, ½H, ½CH), 6.36 (s, ½H, ½CH), 6.89–7.54 (m, 13H, 11ArH + CH), 8.04–8.11 (m, 1H, CH); *m/z* 550 $(M + H)^+$.

*7.1.7. 7-[2-[1-(2-Ethoxycarbonyl-1-phenylethyl)-1H-indol-4-yl]ethyl]-3,4-dihydro-2H-[1,8]naphthyridine-1-carboxylic acid tert-butyl ester (**17**)*

A mixture of **16** (470 mg, 0.86 mmol) and 10% Pd/C (50 mg) in absolute methanol (100 mL) was shaken in a hydrogenation apparatus under atmospheric pressure at room temperature for 20 h. The catalyst was removed by filtration, washed with methanol and the filtrate was concentrated to dryness yielded **17** (466 mg, 98%). ^{1}H NMR (400 MHz, $CDCl_3$) δ 1.01 (t, 3H, CH_3), 1.47 (m, 9H, $(CH_3)_3$), 1.86 (quint., 2H, CH_2), 2.66 (t, 2H, CH_2), 3.03–3.07 (m, 2H, CH_2), 3.21–3.26 (m, 4H, $2CH_2$), 3.69–3.72 (m, 2H, CH_2), 3.97 (m, 2H, CH_2), 6.01 (t, 1H, CH), 6.56 (d, 1H, ArH), 6.71 (d, 1H, ArH), 6.87 (d, 1H, ArH), 7.00–7.04 (m, 1H, ArH), 7.13–7.25 (m, 8H, ArH); *m/z* 554 $(M + H)^+$.

*7.1.8. 3-Phenyl-3-[4-[2-(5,6,7,8-tetrahydro[1,8]naphthyridin-2-yl)ethyl]indol-1-yl]propionic acid (**9**)*

A solution of **17** (315 mg, 1.49 mmol) and copper(II) trifluoromethanesulphonate (23 mg, 0.0447 mmol) in toluene (3 mL) and DMF (0.5 mL) was heated at 130 °C in a microwave oven cavity for 1000 s. After evaporation of the solvent, the residue was chromatographed on silica (AcOEt/CH_2Cl_2/EtOH, 4:5:1) to give 3-phenyl-3-[4-[2-(5,6,7,8-tetrahydro[1,8]-naphthyridin-2-yl)ethyl]indol-1-yl]propionic acid ethyl ester **18** (323 mg, 48%); *m/z* 454 $(M + H)^+$. A solution of **18** (110 mg, 0.245 mmol) and $LiOH \cdot H_2O$ (13 mg, 0.31 mmol) in THF (3 mL), MeOH (1 mL), and H_2O (0.3 mL) was stirred for 26 h at 25 °C. After evaporation of the solvent, the residue was purified by chromatography on silica (CH_2Cl_2/EtOH, 9:1). Recrystallization from EtOH/H_2O yielded **9** (85 mg, 73%) as

colorless prisms. ^{1}H NMR (400 MHz, DMSO-d_6) δ 1.76–1.84 (m, 2H, CH_2), 2.63–2.73 (m, 2H, CH_2), 2.88–2.98 (m, 2H, CH_2), 3.05–3.17 (m, 2H, CH_2), 3.35–3.57 (m, 4H, $2CH_2$), 5.85–6.00 (m, 1H, CH), 6.17–6.21 (m, 1H, ArH), 6.42–6.55 (m, 1H, ArH), 6.60–6.62 (m, 1H, ArH), 6.85 (d, $J = 7.6$, 1H, ArH), 6.98–7.05 (m, 1H, ArH), 7.15–7.42 (m, 6H, ArH), 7.74 (br s, 1H, ArH); *m/z* 426 $(M + H)^+$. HRMS (ESI) *m/z* calcd for $C_{27}H_{27}N_3O_2$ 425.21033, found 426.21254 $(M + H^+)$.

*7.1.9. 7-[2-[1-[2-Methoxycarbonyl-1-(3-pyridyl)vinyl]-1H-indol-4-yl]vinyl]-3,4-dihydro-2H-[1,8]naphthyridine-1-carboxylic acid tert-butyl ester (**19**)*

Product **19** was prepared (84%) from **15** and methyl 3-pyridylpropiolate using the procedure described for **16**. Compound **19** was isolated as an *E/Z* mixture. ^{1}H NMR (400 MHz, $CDCl_3$) δ 1.61 (s, 9H, $(CH_3)_3$), 1.95–2.01 (m, 2H, CH_2), 2.80 (t, 2H, CH_2), 3.62 (s, 2H, 2CH), 3.71 (s, 1H, 1CH), 3.82–3.85 (m, 2H, CH_2), 6.35 (s, 1/3H, 1/3CH), 6.38 (s, 2/3H, 2/3CH), 6.79–7.47 (m, 10H, 8ArH + 2CH), 8.04–8.1 (m, 1H, ArH), 8.69–8.72 (m, 2H, ArH); *m/z* 537 $(M + H)^+$.

*7.1.10. 7-[2-[1-[2-Carboxy-1-(3-pyridyl)ethyl]-1H-indol-4-yl]ethyl]-3,4-dihydro-2H-[1,8]naphthyridine-1-carboxylic acid tert-butyl ester (**20**)*

A solution of **19** (600 mg, 1.12 mmol), $LiOH \cdot H_2O$ (85 mg, 2.03 mmol) and 10% Pd/C (600 mg) in THF (10 mL), MeOH (5 mL), and H_2O (1 mL) was stirred for 2 h at 25 °C. Then, the mixture was shaken in a hydrogenation apparatus under atmospheric pressure of H_2 at room temperature for 24 h. The catalyst was removed by filtration, washed with methanol and the filtrate was concentrated to dryness. Then, the residue was partitioned between ice-cold water (30 mL) and AcOEt (20 mL). The aqueous layer was acidified to pH = 4 with diluted AcOH, then extracted twice with additional AcOEt (2 × 50 mL) and dried (Na_2SO_4). After evaporation of the solvent, the residue was triturated in ether and filtered to give **20** (483 mg, 82%). ^{1}H NMR (400 MHz, $CDCl_3$) δ 1.57 (s, 9H, $(CH_3)_3$), 1.95 (quint., 2H, CH_2), 2.76 (t, 2H, CH_2), 3.08–3.44 (m, 6H, $3CH_2$), 3.78–3.82 (m, 2H, CH_2), 6.16 (t, 1H, CH), 6.64 (d, 1H, ArH), 6.82 (d, 1H, ArH), 6.95 (d, 1H, ArH), 7.08–7.42 (m, 6H, ArH), 8.46–8.47 (m, 1H, ArH), 8.61 (d, 1H, ArH); *m/z* 427 $(M - (t\text{-BOC}) + H)^+$.

*7.1.11. 3-Pyridin-3-yl-3-[4-[2-(5,6,7,8-tetrahydro [1,8]naphthyridin-2-yl)ethyl]indol-1-yl] propionic acid (**21**)*

Compound **21** was prepared (48%) from **20** using the procedure described for **18**. ^{1}H NMR (400 MHz, $CDCl_3$) δ 1.85–1.89 (m, 2H, CH_2), 2.40–2.82 (m, 6H, $3CH_2$), 3.16–3.37 (m, 2H, CH_2), 3.44–3.46 (m, 2H, CH_2), 5.85–6.00 (m, 1H, CH), 6.17–6.21 (m, 1H, CH), 6.32–6.55 (m, 1H, ArH), 6.92 (t, $J = 7.2$, 1H, ArH), 7.02–7.53 (m, 6H, ArH), 8.45–8.48 (m, 2H, ArH), 10.96 (br s, 1H, NH); *m/z* 427 $(M + H)^+$. HRMS (ESI) *m/z* calcd for $C_{26}H_{26}N_4O_2$ 426.20558, found 427.20594 $(M + H^+)$.

*7.1.12. 3-(4-Aminoindol-1-yl)-3-(3-pyridyl) acrylic acid methyl ester (**23**)*

Compound **23** was prepared from **22** and methyl 3-pyridylpropiolate using the procedure described for **19**. Compound **23** was isolated (85%) as a *E/Z* mixture. ^{1}H NMR (400 MHz, $CDCl_3$) δ 3.62 (s, 2H, $2/3CH_3$), 3.69 (s, 1H, $1/3CH_3$), 6.28–6.82 (m, 4H, 3ArH + CH), 6.90 (t, $J = 8.2$, 1H, ArH), 7.03 (d, $J = 3.6$, 1H, ArH), 7.25–7.29 (m, 1H, ArH), 7.35–7.47 (m, 1H, ArH), 8.67–8.75 (m, 2H, ArH); *m/z* 294 $(M + H)^+$.

*7.1.13. 7-[[1-[2-Methoxycarbonyl-1-(3-pyridyl) vinyl]-1H-indol-4-ylamino]methyl]-3,4-dihydro-2H-[1,8]naphthyridine-1-carboxylic acid tert-butyl ester (**24**)*

A mixture of **23** (200 mg, 0.68 mmol), **13** (215 mg, 0.82 mmol), sodium triacetoxyborohydride (260 mg, 1.2 mmol), and acetic acid (47 μL, 0.82 mmol) in 1,2-dichloroethane was stirred at room temperature for 12 h. After evaporation of the solvent, the residue was purified by chromatography on silica (AcOEt) yielded **24** (264 mg, 72%) as an *E/Z* mixture. ^{1}H NMR (400 MHz, $CDCl_3$) δ 1.56 (s, 9H, $3CH_3$), 1.95–2.01 (m, 2H, CH_2), 2.77–2.82 (m, 2H, CH_2), 3.26–3.43 (m, 2H, CH_2), 3.61 (s, 2H, $2/3CH_3$), 3.92 (s, 1H, $1/3CH_3$), 3.79–3.86 (m, 2H, CH_2), 4.55 (br s, 4/3H, $4/3CH_2$), 4.71 (br s, 2/3H, $2/3CH_2$), 6.28–6.35 (m, 2H, 1ArH + 1CH), 6.80–7.06 (m, 4H, ArH), 7.27–7.31 (m, 1H, ArH), 7.40 (d, $J = 7.6$, 1H, ArH), 7.43–7.48 (m, 2H, ArH), 8.68–8.71 (m, 2H, ArH); *m/z* 540 $(M + H)^+$.

*7.1.14. 7-[[1-[2-Carboxy-1-(3-pyridyl)ethyl]-1H-indol-4-ylamino]methyl]-3,4-dihydro-2H-[1,8]naphthyridine-1-carboxylic acid tert-butyl ester (**25**)*

Compound **25** was prepared (73%) from **24** using the procedure described for **20**. ^{1}H NMR (400 MHz, $CDCl_3$) δ 1.55 (s, 9H, $3CH_3$), 1.92–2.00 (m, 2H, CH_2), 2.74–2.80 (m, 2H, CH_2), 3.26–3.43 (m, 2H, CH_2), 3.79–3.86 (m, 2H, CH_2), 4.35 (dd, $J = 16.4$, $J = 32.0$, 2H, CH_2), 6.12–6.15 (m, 2H, 1ArH + 1CH), 6.69 (d, $J = 3.2$, 1H, ArH), 6.72 (d, $J = 8.8$, 1H, ArH), 6.96–7.03 (m, 2H, ArH), 7.22–7.24 (m, 2H, ArH), 7.36–7.41 (m, 2H, ArH), 8.46 (d, $J = 4.4$, 1H, ArH), 8.60 (s, 1H, ArH); *m/z* 528 $(M + H)^+$.

*7.1.15. 3-(3-Pyridyl)-3-[4-[[(5,6,7,8)-tetrahydro [1,8]naphthyridin-2-yl methyl]amino] indol-1-yl]propionic acid (**26**)*

Compound **26** was prepared from **25** using the procedure described for **21**. ^{1}H NMR (400 MHz, $MeOD_4$) δ 1.70–1.85 (m, 2H, CH_2), 2.61–2.70 (m, 2H, CH_2), 3.17–3.30 (m, 2H, CH_2), 4.27 (dd, $J = 16.4$, $J = 31.6$, 2H, CH_2), 5.97 (d, $J = 7.6$, 1H, ArH), 6.11 (t, $J = 4.4$, 1H, CH), 6.59 (d, 1H, ArH), 6.66–7.42 (m, 6H, ArH), 7.64–7.67 (m, 1H, ArH), 8.36 (d, $J = 2.4$, 2H, ArH); *m/z* 428 $(M + H)^+$. HRMS (ESI) *m/z* calcd for $C_{25}H_{25}N_5O_2$ 427.20083, found 428.20875 $(M + H^+)$.

7.2. Pharmacology

7.2.1. $\alpha_{IIb}\beta_{IIIa}$-Fibrinogen assay

The assay is based on the method of Dennis [30]. Costar 9018 flat-bottom 96-well ELISA plates were coated overnight at 4 °C with 100 μL/well of 10 μg/mL human fibrinogen (Calbiochem) in 20 mM Tris–HCl pH 7.5, 150 mM NaCl, 2 mM $CaC1_2$, 0.02% NaN_3 (TAC buffer). Plates were subsequently emptied and blocked for 1 h at 37 °C with 150 μL/well of TAC buffer containing 0.05% Tween 20 and 1% bovine serum albumin (TACTB buffer). After washing 3 times with 300 μL/well of 10 mM Na_2HPO_4 pH 7.5, 150 mM NaCl, 0.01% Tween 20 (PBST buffer), controls or test compound (0.027–20.0 μM) were mixed with 40 μg/mL human GPIIbIIIa (Enzyme Research Laboratories) in TACTB buffer, and 100 μL/well of these solutions were incubated for 1 h at 37 °C. The plate was then washed 5 times with PBST buffer, and 100 μL/well of a monoclonal anti-GPIIbIIIa antibody in TACTB buffer (1 μg/mL, Enzyme Research Laboratories) and was incubated at 37 °C for 1 h. After washing 5 times with PBST buffer and 100 μL/well of goat anti-mouse IgG conjugated to horseradish peroxidase (Kirkegaard & Perry) and was incubated at 37 °C for 1 h (25 ng/mL in PBST buffer), followed by a 6-fold PBST buffer wash. The plate was developed by adding 100 μL/well of 0.67 mg *o*-phenylenediamine dihydrochloride per milliliter of 0.012% H_2O_2, 22 mM sodium citrate, 50 mM sodium phosphate, pH 5.0 at room temperature. The reaction was stopped with 50 μL/well of 2 M H_2SO_4, and the absorbance at 492 nm was recorded. Percent (%) inhibition was calculated from an average of three separate determinations relative to buffer controls (no test compound added), and a four parameter fit was used to estimate the half maximal inhibition concentration (IC_{50}).

7.2.2. $\alpha_v\beta_3$-Vitronectin assay

The assay was based on the method of Niiya [31], and all steps were performed at room temperature. Costar 9018 flat-bottom 96-well ELISA plates were coated overnight at room temperature with 100 μL/well of 0.4 μg/mL human $\alpha_v\beta_3$ (Chemicon) in TS buffer (20 mM Tris–HCl pH 7.5, 150 mM NaCl, 1 mM $CaCl_2$, 1 mM $MgCl_2$, 1 mM $MnCl_2$). Plates were subsequently emptied and blocked for 2 h with 150 μL/well of TS buffer containing 1% BSA (TSB buffer), and washed 3 times with 300 μL/well of PBST buffer. Controls or test compound (0.0001–20.0 μM) were mixed with 1 μg/mL of human vitronectin (Chemicon) that had been biotinylated in-house with sulfo-NHS-LC-LC-biotin (Pierce, 20:1 molar ratio), and 100 μL/well of these solutions (in TSB buffer) were incubated for 2 h. The plate was then washed 5 times with PBST buffer, and 100 μL/well of 0.25 μg/mL NeutrAvidin-horseradish peroxidase conjugate (Pierce) in TSB buffer was added to the plate and incubated for 1 h. Following a 5-fold PBST buffer wash, the plate was developed and results were calculated as described for the IIbIIIa-fibrinogen assay.

7.2.3. $\alpha_v\beta_5$-Vitronectin assay

The assay is similar to the $\alpha_v\beta_3$-vitronectin assay, and all steps were performed at room temperature. Costar 9018 flat-botom 96-well ELISA plates were coated overnight at room temperature with 100 μL/well of 1 μg/mL human $\alpha_v\beta_5$ (Chemicon) in TS buffer. Plates were blocked for 2 h with 150 μL/well of TSB buffer, and washed 3 times with 300 μL/well of PBST buffer. Controls or test compound (0.0001–20 μM) were mixed with 1 μg/mL of human vitronectin (Chemicon) that had been biotinylated in-house with sulfo-NHS-LC-LC-biotin (Pierce, 20:1 molar ratio), and 100 μL/well of these solutions (in TSB buffer) were incubated for 2 h. The plate was then washed 5 times with PBST buffer, and 100 μL/well of 0.25 μg/mL NeutrAvidin-horseradish peroxidase conjugate (Pierce) in TSB buffer was added to the plate and incubated at for 1 h. Following a 5-fold PBST buffer wash, the plate was developed and results were calculated as described for the IIbIIIa-fibrinogen assay.

7.2.4. $\alpha_5\beta_1$-Fibronectin assay

Costar 9018 flat-botom 96-well ELISA plates were coated overnight at room temperature with 100 μL/well of 3 μg/mL human $\alpha_5\beta_1$ (Chemicon) in TS buffer. Plates were subsequently emptied and blocked for 2 h at 30 °C with 150 μL/well of TSB buffer, and washed 3 times with 300 μL/well of PBST buffer. Controls or test compound (0.0001–20 μM) were mixed with 1 μg/mL of human fibronectin (Chemicon) that had been biotinylated in-house with sulfo-NHS-LC-LC-biotin (Pierce, 20:1 molar ratio), and 100 μL/well of these solutions (in TSB buffer) were incubated for 2 h at 30 °C. The plate was then washed 3 times with PBST buffer, and 100 μL/well of 0.25 μg/mL NeutrAvidin-horseradish peroxidase conjugate (Pierce) in TSB buffer was added to the plate and incubated at for 1 h at 30 °C. Following a 6-fold PBST buffer wash, the plate was developed and results were calculated as described for the IIbIIIa-fibrinogen assay.

References

[1] (a) M. Yamamoto, J.E. Fisher, M. Gentile, J.G. Seedor, C.-T. Leu, S.B. Rodan, G.A. Rodan, Endocrinology 139 (1998) 1411;
(b) V.W. Engleman, G.A. Nickols, F.P. Ross, M.A. Horton, D.W. Griggs, S.L. Settle, P.G. Ruminski, S.L. Teitelbaum, J. Clin. Invest. 99 (1997) 2284–2292;
(c) M.W. Lark, G.B. Stroup, S.M. Hwang, I.E. James, D.J. Rieman, F.H. Drake, J.N. Bradbeer, A. Mathur, K.F. Erhard, K.A. Newlander, S.T. Ross, K.L. Salyers, B.R. Smith, W.H. Miller, W.F. Huffman, M. Gowen, J. Pharmacol. Exp. Ther. 291 (1999) 612–617;
(d) S.J. Hoffman, J. Vasko-Moser, W.H. Miller, M.W. Lark, M. Gowen, G. Stroup, J. Pharmacol. Exp. Ther. 302 (2002) 205;
(e) J.E. Fisher, M.P. Caulfield, M. Sato, H.A. Quartuccio, R.J. Gould, V.M. Garsky, G.A. Rodan, M. Rosenblatt, Endocrinology 132 (1993) 1411–1413.
(f) G.D. Hartman, M.E. Duggan, Expert Opin. Investig. Drugs 9 (2000) 1281–1291;
(g) B.A. Crippes, V.W. Engleman, S.L. Settle, J. Delarco, R.L. Ornberg, M.H. Helfrich, M.A. Horton, G.A. Nickols, Endocrinology 137 (1996) 918–924.
(h) T.J. Chambers, K. Fuller, J.A. Darby, J.A.S. Pringel, M.A. Horton, Bone Miner. 1 (1986) 127–135.
[2] C.M. Storgard, D.G. Stupack, A. Jonczyk, S.L. Goodman, R.I. Fox, D.A. Cherresh, J. Clin. Invest. 103 (1999) 47–54.
[3] R. Haubner, D. Finsinger, H. Kessler, Angew. Chem. Int. Ed. Engl. 36 (1997) 1374–1389.

[4] (a) J.D. Hood, D.A. Cheresh, Nat. Rev. Cancer 21 (2002) 91–100;
(b) G.C. Tucker, Curr. Opin. Pharmacol. 2 (2002) 394–402;
(c) J.A. Varner, D.A. Cheresh, Curr. Opin. Cell Biol. 8 (1996) 724–730;
(d) P.C. Brooks, A.M.P. Montgomery, M. Rosenfeld, R.A. Reisfeld, T. Hu, G. Klier, D.A. Cheresh, Cell 79 (1994) 1157–1164;
(e) G.J. Mizejewski, Proc. Soc. Exp. Biol. Med. 222 (1999) 124–138;
(f) J. Samanen, Z. Jonak, D. Rieman, T.L. Yue, Curr. Pharm. Des. 3 (1997) 545–584.
[5] F. Mitjans, T. Meyer, C. Fittschen, S. Goodman, A. Jonczyk, J.F. Marshall, G. Reyes, J. Piulats, Int. J. Cancer 87 (2000) 716–723.
[6] L.A. Sorbera, A. Graul, J. Castañer, Drugs Future 25 (2000) 674–678.
[7] A.M. Badger, S. Blake, R. Kapadia, S. Sarkar, J. Levin, B.A. Swift, S.J. Hoffman, G.B. Stroup, W.H. Miller, M. Gowen, M.W. Lark, Arthritis Rheum. 44 (2001) 128–137.
[8] J.J. Marugán, C. Manthey, B. Anaclerio, L. LaFrance, T. Lu, T. Markotan, C. Crysler, S. Eisennagel, M. Dasgupta, B. Tomczuk, J. Med. Chem. 48 (2005) 926–934.
[9] K. Leonard, W. Pan, B. Anaclerio, J.M. Gushue, Z. Guo, R.L. DesJarlais, J. Lattanze, C. Crysler, C.L. Manthey, B.E. Tomczuk, J.J. Marugan, Bioorg. Med. Chem. Lett. 15 (2005) 2679–2684.
[10] L. Marinelli, A. Lavecchia, K.-E. Gottschalk, E. Novellino, H. Kessler, J. Med. Chem. 46 (2002) 4393–4404.
[11] J.-P. Xiong, T. Stehle, R. Zhang, A. Joachimiak, M. Frech, S.L. Goodman, M. Arnaout, Science 296 (2002) 151–155.
[12] H.M. Berman, J. Westbrook, Z. Feng, G. Gary Gilliland, T.N. Bhat, H. Weissig, I.N. Shindyalov, P.E. Bourne, Nucleic Acids Res. 28 (2000) 235–242.
[13] F. Mohamadi, N.G.J. Richards, W.C. Guida, R. Liskamp, M. Lipton, C. Caufield, G. Chang, T. Hendrickson, W.C. Still, J. Comput. Chem. 11 (1990) 440–467.
[14] T.A. Halgren, J. Comput. Chem. 17 (1996) 490–519.
[15] T.A. Halgren, J. Comput. Chem. 17 (1996) 520.
[16] T.A. Halgren, J. Comput. Chem. 17 (1996) 553–586.
[17] T.A. Halgren, J. Comput. Chem. 17 (1996) 587–615.
[18] T.A. Halgren, R. Nachbar, J. Comput. Chem. 17 (1996) 616–641.
[19] T.A. Halgren, J. Comput. Chem. 20 (1999) 720–729.
[20] T.A. Halgren, J. Comput Chem. 20 (1999) 730–748.
[21] Accelrys, San Diego, CA, <http://www.accelrys.com/>, 2001.
[22] M.J.S. Dewar, E.G. Zoebisch, E.F. Healy, J.J.P. Stewart, J. Am. Chem. Soc. 107 (1985) 3902–3909.
[23] Wavefunction, Irvine, CA,<http://www.wavefun.com>, 1999.
[24] M. Pfaff, K. Tangemann, B. Muller, M. Gurrath, G. Muller, H. Kessler, R. Timpl, J. Engel, J. Biol. Chem. 269 (1994) 20233–20238.
[25] K. Burgess, D. Lim, S.A. Mousa, J. Med. Chem. 39 (1996) 4520–4526.
[26] W.H. Miller, D.P. Alberts, P.K. Bhatnagar, W.E. Bondinell, J.F. Callahan, R.R. Calvo, R.D. Cousins, K.F. Erhard, D.A. Heerding, R.M. Keenan, C. Kwon, P.J. Manley, K.A. Newlander, S.T. Ross, J.M. Samanen, I.N. Uzinskas, J.W. Venslavsky, C.C.-K. Yuan, R.C. Haltiwanger, M. Gowen, S.-W. Hwang, I.E. James, M.W. Lark, D.J. Rieman, G.B. Stroup, L.M. Azzarano, K.L. Salyers, B.R. Smith, K.W. Ward, K.O. Johanson, W.F. Huffman, J. Med. Chem. 43 (2000) 22–26.
[27] M.E. Duggan, J.H. Hutchinson, Expert Opin. Ther. Patents 10 (2000) 1367–1385.
[28] P.J. Coleman, L.T. Duong, Expert Opin. Ther. Patents 12 (2002) 1009–1021.
[29] T. Lu, L.V. Lafrance, T.P. Markotan, J.J. Marugan, V.J. Marder, D.C. U'Prichard, B.M. Anaclerio, Z. Guo, W. Pan, K.A. Leonard, WO 2002060438.
[30] M.S. Dennis, P. Carter, R.A. Lazarus, Proteins 15 (1993) 312–321.
[31] K. Niiya, E. Hodson, R. Bader, V. Byers-Ward, J.A. Koziol, E.F. Plow, Z.M. Ruggeri, Blood 70 (1987) 475–483.
[32] S. Yamashita, K. Konishi, Y. Yamazaki, Y. Taki, T. Sakane, H. Sezaki, Y. Furuyama, J. Pharm. Sci. 91 (2002) 669–679.
[33] R.S. Obach, J.G. Baxter, T.E. Liston, M. Silber, B.C. Jones, F. MacIntire, D.J. Rance, P. Wastall, J. Pharmacol. Exp. Ther. 283 (1997) 46–58.